

Estimating the Concentration of Soil Heavy Metals in Agricultural Areas from AVIRIS Hyperspectral Imagery

Sangeetha Annam¹, Anshu Singla²

Submitted: 20/10/2022

Revised: 24/12/2022

Accepted: 23/01/2023

Abstract: Heavy metal contamination in agricultural soil is currently a global issue. The traditional approaches for soil heavy metal (HM) estimation are insufficient for large-scale and in-time monitoring and assessment. AVIRIS hyperspectral imaging can be utilized in better way to estimate HM concentrations in soil. The authors employed transfer learning model to classify the images, further HM concentration estimation was compared with the actual values. Experimental findings show VGG19 outperformed other deep learning and machine learning models and yielded a consistent accuracy of 81.25% starting from epoch 134 to 200 epochs. The root means square error (RMSE) values of different heavy metals, arsenic (As), cadmium (Cd) and lead (Pb) were found to be 2.89, 0.12, and 0.22 and the mean square value (MSE) value was evaluated to be 0.96, 0.01, and 0.04, respectively. The results of HM estimation proves that the proposed technique is efficient and effective.

Keywords: AVIRIS satellite images, Soil HM concentration, Correlated bands, Transfer Learning Models.

1. Introduction

Soil, considered to be the vital component of the ecosystem, directly affects the creature's health. Many human activities, which include wastewater, parent materials, sewage sludge, and the irrational use of pesticides, are the sources of soil heavy metals (HM). HM crop enrichment poses a major hazard to human life and health. In recent years, hyperspectral images (HSIs) have grown in popularity for acquisition, analysis, and application as remote sensing observation technology has advanced. This captures the weak discriminative features of HM due to their abundant spectral information. Most studies that concentrate on estimation of soil HM via remote sensing (RS) have focused on the visible–near-infrared (VNIR) region [1] of the spectrum (i.e., 350–2500 nm), with the mid-infrared (MIR) and far-infrared (FIR) wavelengths being employed significantly less frequently. This is because the visible–near-infrared spectrum contains soil characteristics and hundreds of sensors that capture a plethora of information.

Major properties of ground objects are revealed rapidly in the restricted spectral ranges of HSI. In general, HSI comprises of contiguous spectral bands where the data redundancy and correlation are higher, which leads to the

"Curse of dimensionality". Unlike multispectral images (MSI), HSIs also extract data from a set of contiguous spectral bands, allowing for better feature extraction and object detection. So, there is a need to reduce the spectral characteristics while preserving the most vital information in classification [2] from HSIs. However, the HSI classification is difficult due to the restricted datasets, multi-dimensional characteristics, bands that are strongly connected, and mixed spectral and spatial information [3]. Nowadays, the widely used method for estimating HM in soil is to employ ground HSI data, which involves pre-treatment of spectral characteristics, spectrum augmentation, feature selection, and modelling [4]. Because, soil has low HM content, preprocessing the spectra to increase weak spectral information is required. Since the 1990s, lab-based techniques including Inductively Coupled Plasma Spectrometry [5], Optical Emission Spectroscopy [6], and Atomic Absorption Spectrometry [7] have been the standards for detecting HM. Several studies investigating the relationship between HSI data and HM contamination in agricultural soil have been conducted in recent years, including Lead (Pb), Cadmium (Cd), Arsenic (As), Chromium (Cr), and Zinc (Zn) using lab-processed soil and HSI data while using numerous learning approaches [8]. The estimation of heavy metals using hyperspectral images can be done using the methods: i) pollution index, ii) enrichment factor, iii) ecological risk index, iv) environmental risk index, v) spectral unmixing of linear mixing model, vi) geo-accumulation index and many more.

^{1,2}Chitkara University Institute of Engineering and Technology
Chitkara University Punjab, India
a.sangeeta@chitkara.edu.in
anshu.singla@chitkara.edu.in

The two important approaches used in hyperspectral images are extraction and selection of features. The former process includes the transformations to transfer the original space onto a lower dimensional plane. During this process, a few features are degraded, affecting their physical interpretation. The later picks an ideal subset that reflects the original space keeping physical interpretation of the original HSI, also known as the band selection method, which is preferred over the feature extraction process on HSIs. Feature selection is categorised into supervised and unsupervised based on the label of the data. Supervised approaches require labelled data, and they frequently use criteria selection through classification performance to select the most informative bands. Unlabelled data, on the other hand, was classified using unsupervised methods. i.e., no prior knowledge of the class samples is required as the methods will neither require the class measures nor the classification accuracy obtained during band selection. Despite the higher classification accuracies provided by supervised algorithms, unsupervised band selection approaches are

preferred as there is more scarcity when compared to unlabelled data [9]. Nowadays, deep convolutional neural network (DCNN) models perform better for classifying hyperspectral image data.

1.1 Estimation of Heavy Metal using Geo-accumulation Index (I_{geo})

The images thus classified are estimated for heavy metal concentration using geo-accumulation index. This index [59] calculates a single metal concentration to determine the pollution degree as an important parameter using the equation mentioned below:

$$I_{geo} = \log_2 [C_n / (K * B_n)] \quad (1)$$

where C_n is the metal concentration, and B_n is the metal's background concentration. k is 1.5 in our experiment, as the background factor. In Table 1, the threshold values of I_{geo} concentration levels were grouped for different classes and the subsequent Section 2 will help us to know the techniques applied over the hyperspectral images for estimation of heavy metals.

Table 1: Geo-accumulation index threshold value

Classes	I_{geo} calculated values (Metal concentration)
0	Less than zero (No contamination)
I	0 to 1 (No to Moderate contamination)
II	1 to 2 (Moderate contamination)
III	2 to 3 (Moderate to Heavy contamination)
IV	3 to 4 (Heavy contamination)
V	4 to 5 (Heavy to Extreme contamination)
VI	Greater than five (Extreme contamination)

The goal of this research is to provide a unique technique for spectral image analysis. In this paper, the authors proposed an efficient model for the estimation of heavy metal concentration with transfer learning models for classification and a geo-accumulation index (I_{geo}) for estimation. The proposed technique is based on the application of transfer learning models that recreate the original features effectively with the help of limited features. The advantage of the suggested approach is that it allows for the detection and extraction of significant information while preserving data of spatial and spectral features. Moreover, it improves HSI classification even when there is a limited number of labelled samples. In addition to this, assimilating multi-objective variables to increase the accuracy of soil heavy metal stress levels based on the following factors: **i)** Fractional abundance determines the abundance i.e. spectral unmixing of the

component materials or endmembers, as the images are selected accordingly; **ii)** calculating the reconstruction error, or the distance between the field and the estimated values; **iii)** Feature Selection (Selection of highly correlated bands), **iv)** increased pixel density; and **v)** estimating heavy metal concentration using the geo-accumulation index. The rest of the paper is structured as follows: Section 2 describes the existing state-of-art literature of estimating heavy metals, Section 3 describes the proposed methodology for estimation of heavy metals, Section 4 describes the dataset and its spectral profiles, Section 5 describes experimental results, and finally conclusion and future work is discussed in Section 6.

2. Existing State-of-Art Literature of Estimating Heavy Metals

In [10], the authors describe a four-layer CNN model for soil detection on eighty synthetic hyperspectral bands and the WorldView-2 satellite's original eight multispectral bands. This significant improvement implies that the performance of the proposed model was improved by utilising pan sharpened HSI bands. In one study [11], the researchers proposed a new crop/weed identification system that combines fine-tuning pre-trained convolutional networks with "traditional" machine learning classifiers and with previously deep extracted features. In [12], the CNN technique was used for

classification with a training and validation accuracy of 99.86% and 97.68%, respectively. For study comparison, most Deep Learning models were trained with ResNet152V2 with an accuracy of 99.15%, VGG16 with 97.58%, VGG19 with 98.44%, InceptionResNetV2 with 98.15%, Xception with 98.86%, and Densenet201 with 98.58%, respectively. In [13], the performance of multivariate HSI vegetation indices was applied to estimate the arsenic content in agricultural soils. In [14], the Geo-accumulation (I_{geo}) and the potential ecological risk (PER) index methods were used to assess the mine dump's heavy metal pollution for Cu, Pb, Cd, As, Zn, and Cr. Table 2 shows the summary of models used for estimating heavy metal concentrations.

Table 2: Various models employed for heavy metal estimation in the existing literature

References	Models	Type of soil data	As	Cu	Pb	Cr	Zn	Ag	Cd
[13]	Successive projection algorithm	Rice data	√					√	
[14]	I_{geo} and PER index method	Mine's topsoil	√	√	√	√	√		√
[15]	I_{geo} and PER index method	Soil near river watershed		√	√	√	√		
[16]	I_{geo} index method	Sediments near seacoast		√	√	√			√
[17]	I_{geo} index	Agricultural soil	√						

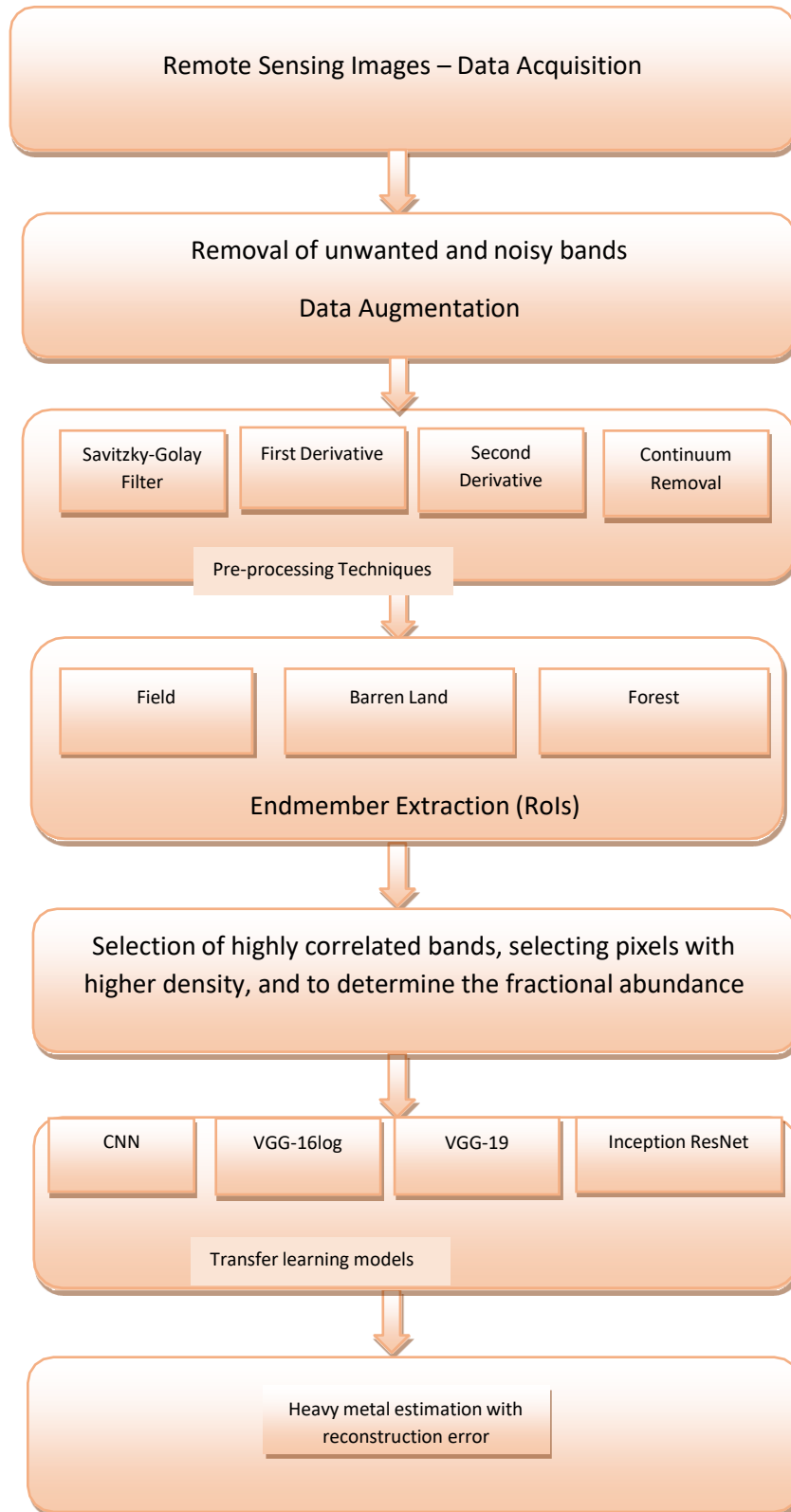
In one of the papers, convolutional neural networks (CNN) [17] is a peculiar method considered in deep learning which allows to build and train the systems. The CNN layers are an important constituent for feature extraction, with an adequate number of layers. Various convolutional models such as VGG16 [22-23], InceptionResNetV2 [24] and VGG19 [25] consumes less power with RMSprop optimizer during computation were compared during the classification process. The best suit of training models to yield the highest classification accuracy over the HSI data are discussed. At first, the HSIs are trained, various classification techniques were employed, and the results are analysed for the best classification accuracy.

3. Proposed Methodology for Estimation of Heavy Metals

To begin, the dataset was stabilised by performing an image augmentation process on three-class samples. Then the remote sensing images were resized and then balanced to be of the same resolution. It was, then expected in this

work that using AVIRIS data with a classification-based algorithm on agricultural soil would produce significant correlation and outcomes that are comparable to the best models (using less noisy data) used in the literature. Second, by utilising endmembers, high-risk agricultural soil could be recognised using reasonable metrics. Third, it is expected that using spectral preprocessing, and data augmentation will help improve the baseline models' accuracy. Fourth, a comparison of a few of the transfer learning models to achieve maximum classification accuracy. Finally, we used I_{geo} to estimate the heavy metal concentration. Overall, this work was successful in identifying an effective technique with multi-objective variables using remote sensing hyperspectral images that provides a nonetheless accurate alternative method for arsenic, cadmium, and lead contamination detection. The collected data was from publicly available sources, and the algorithms were written in Python. Figure 1 depicts a workflow of all the major steps of the proposed methodology.

Fig. 1 Workflow diagram for heavy metal estimation from hyperspectral satellite data

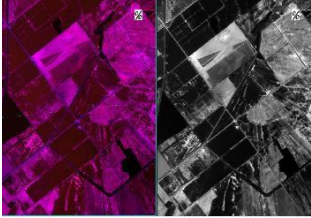
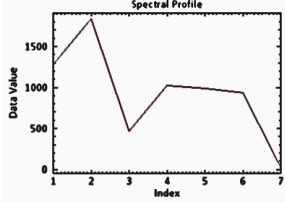
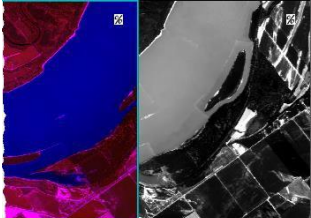
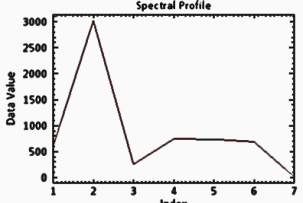


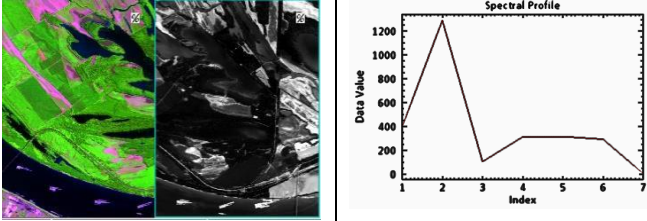
4. Dataset and its Spectral Profiles

The study region is one of the country's most important regions of the USA and is acquired from the URL: https://aviris.jpl.nasa.gov/data/free_data.html. This region is situated in 36°19'N latitude and 121°15'W longitude, respectively. This agricultural region receives an average rain of 23 inches, average snow of 0 inches, an average of 265 sunny days, and receives precipitation 56 days per year. The number of sunny days is 205 and receives more rain than other localities in California, with an annual rainfall of 23.1 inches.

The samples collected, were estimated for heavy-metal content in this region at regular intervals of time which avoids soil degradation, crop yield reduction, and human health issues. For the top layer of soil, publicly available data for soil HM concentration in agricultural lands (in mg/kg) were estimated. Soil As, Pb and Cd heavy metal estimation for agricultural soil with the AVIRIS hyperspectral data and their respective spectral profiles and basic statistical measures are shown in Table 3.

Table 3: Spectral profile of As, Cd and Pb for greyscale and composite images with their statistical measures

Composite and Grayscale image	Spectral Profile of the composite image	Statistical Measures of false colour composite image				
		Min	Max	Mean	SD	
<p>Arsenic</p> 		<p>Band 1 360 20041.00</p> <p>Band 2 0 19692.62</p> <p>Band 3 21 20218.65</p> <p>Band 4 41 20077.98</p> <p>Band 5 38 20082.79</p> <p>Band 6 34 20097.87</p> <p>Band 7 0 20313.48</p>	65536	65536	7874.89	
<p>Cadmium</p> 		<p>Band 1 459 19327.32</p> <p>Band 2 6 19008.65</p> <p>Band 3 16 19514.66</p> <p>Band 4 26 19418.17</p> <p>Band 5 24 19419.43</p> <p>Band 6 21 19430.11</p> <p>Band 7 0 19572.58</p>	65536	65536	7251.17	

Lead		Min	Max	Mean	SD
		Band 1	299	65486	9221.73
			21870.26		
		Band 2	167	65486	9827.98
			21643.98		
		Band 3	9	65486	8752.08
			22049.96		
		Band 4	17	65486	8978.47
		21963.22			
	Band 5	16	65486	8970.64	
		21966.13			
	Band 6	12	65486	8945.41	
		21975.76			
	Band 7	0	65535	8713.78	
		22228.98			


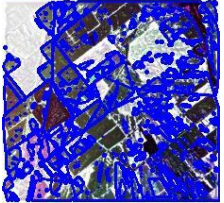

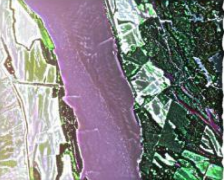
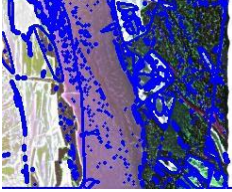
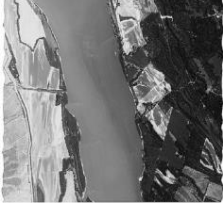

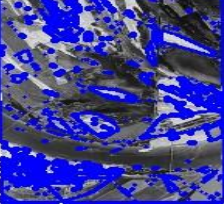

5. Experimental Results

5.1 Glimpses of the images obtained after pre-processing

Several enormous studies inferred that HSI is to be pre-processed using geometrically or atmospherically corrective corrections before applying any model or algorithm. Three views of the HSI during preprocessing

steps are shown in Table 5. The original images are sharpened using the bicubic interpolation technique [18] under geometric correction [19] in the preprocessing step. To minimise the scatter correction on the HSI data, a convex hull [20] is used. Table 4 shows glimpses of the pre-processed images obtained.

Table 4: Pre-processed images for different heavy metals

Heavy Metal	Sharpened Image, alpha = 10	Convex Hull Image	Flatten Image	Greyscale
Arsenic	Sharpened image, alpha=10 			
Cadmium	Sharpened image, alpha=10 			
Lead	Sharpened image, alpha=10 			

5.2 Classification using the Transfer Learning Model

The following section describes the best suit of training models to yield the highest classification accuracy over the HSI data. The VGG19 transfer learning model, which

was tuned with the Adam optimizer and sparse_categorical_crossentropy_loss, performed better than the other Deep Learning Models. Table 5 summarises the results obtained from different deep learning models.

Table 5: Deep Learning Model comparison for classification

Models employed	Train_accuracy	Train_precision	Train_recall	Val_accuracy	Val_precision	Val_recall
CNN	0.9216	0.9296	0.8627	0.5556	0.5556	0.5556
Aug CNN	0.9688	0.9739	0.9634	0.487	0.4821	0.4696
VGG16log	0.5576	0.6305	0.4316	0.5966	0.6543	0.4454
InceptionResnetV2	0.5576	0.6305	0.4316	0.5966	0.6543	0.4454
VGG19	0.9923	0.9945	0.9422	0.8125	0.8234	0.7626

The images thus classified are estimated for heavy metal concentration using the various estimation models discussed above. These indices [26] calculates a single metal concentration to determine the pollution degree as an important parameter. After classification of the hyperspectral images using the pre-trained transfer learning models, the last step of this research work is to estimate the heavy metal concentration of arsenic,

cadmium and lead using geo-accumulation index. Further, Table 6 signifies the geo-accumulation index factor of the field and estimated values of heavy metals for the agricultural soil under consideration. As the calculated geo-accumulation index value is less than zero for field value and estimated value implies that the region is uncontaminated.

Table 6: Comparison of the field and estimated values for different heavy metals

Heavy Metal	Standard Limit	Spectral value		Calculated value	
		Field	Estimated	Field	Estimated
Arsenic	20	14.4	15.33	-1.0588	-0.9686
Cadmium	3	3.47	3.45	-0.3749	-0.3833
Lead	100	6.69	6.73	-4.4868	-4.4782

6. Conclusion and Future work

This article proposed a framework to determine heavy metal estimation in agricultural soils, which was assessed using the NASA AVIRIS dataset. Pre-processing of the HSI involves removal of the noisy bands and duplicate images, resizing of images, and applying atmospheric correction methods. highly correlated bands, selection of pixels with higher density, and feature extraction. One of the transfer learning models, VGG19, yields the maximum R² accuracy percentage as compared with the other deep learning models. The RMSE for arsenic, cadmium, and lead were found to be exceptionally low, which suggests that the observed and simulated values are

close enough to be accurate. Also, while computing the heavy metal concentration using the geo-accumulation index (I_{geo}), the area under consideration was found to be uncontaminated. This work will serve the purpose of allowing government officials to take the necessary steps to estimate heavy metal concentration. Future work can be focused on improving the model's optimization performance by adding more features or by altering the parameters to acquire a separate set of features to yield better results.

References

- [1] P. Fu *et al.*, "A new three-band spectral and metal element index for estimating soil arsenic content

- around the mining area,” *Process Saf. Environ. Prot.*, vol. 157, pp. 27–36, 2022.
- [2] I. M. Simpson, R. J. Winston, and M. R. Brooker, “Effects of land use, climate, and imperviousness on urban stormwater quality: A meta-analysis,” *Sci. Total Environ.*, vol. 809, p. 152206, 2022.
- [3] H. Zhang, L. Wang, T. Tian, and J. Yin, “A review of unmanned aerial vehicle low-altitude remote sensing (UAV-LARS) use in agricultural monitoring in China,” *Remote Sens.*, vol. 13, no. 6, p. 1221, 2021.
- [4] S. Ding, X. Zhang, W. Sun, K. Shang, and Y. Wang, “Estimation of soil lead content based on GF-5 hyperspectral images, considering the influence of soil environmental factors,” *J. Soils Sediments*, pp. 1–15, 2022.
- [5] M. Zaeem *et al.*, “Development of a hyperspectral imaging technique using LA-ICP-MS to show the spatial distribution of elements in soil cores,” *Geoderma*, vol. 385, p. 114831, 2021.
- [6] Y. Fu *et al.*, “An overview of crop nitrogen status assessment using hyperspectral remote sensing: Current status and perspectives,” *Eur. J. Agron.*, vol. 124, p. 126241, 2021.
- [7] S. Arianto, A. H. Saputro, T. Ernawati, I. Isnaeni, C. Imawan, and D. Djuhana, “Rapid Detection of Cadmium Concentration in Beche-de-mer Using Hyperspectral Imaging Technology and Deep Neural Networks Regression Technique,” in *2021 IEEE 5th International Conference on Information Technology, Information Systems and Electrical Engineering (ICITISEE)*, 2021, pp. 30–34.
- [8] X. Zhou, J. Sun, Y. Tian, K. Yao, and M. Xu, “Detection of heavy metal lead in lettuce leaves based on fluorescence hyperspectral technology combined with deep learning algorithm,” *Spectrochim. Acta Part A Mol. Biomol. Spectrosc.*, vol. 266, p. 120460, 2022.
- [9] R. Zaatour, S. Bouzidi, and E. Zagrouba, “Impact of Feature Extraction and Feature Selection Techniques on Extended Attribute Profile-based Hyperspectral Image Classification,” in *VISIGRAPP (4: VISAPP)*, 2017, pp. 579–586.
- [10] Lu, Y., Perez, D., Dao, M., Kwan, C., & Li, J. (2018, November). Deep learning with synthetic hyperspectral images for improved soil detection in multispectral imagery. In *2018 9th IEEE Annual Ubiquitous Computing, Electronics & Mobile Communication Conference (UEMCON)* (pp. 666-672). IEEE.
- [11] Espejo-Garcia, B., Mylonas, N., Athanasakos, L., Fountas, S., & Vasilakoglou, I. (2020). Towards weeds identification assistance through transfer learning. *Computers and Electronics in Agriculture*, 171, 105306.
- [12] Lanjewar, M. G., & Gurav, O. L. (2022). Convolutional Neural Networks based classifications of soil images. *Multimedia Tools and Applications*, 81(7), 10313-10336.
- [13] Shi, T., Liu, H., Chen, Y., Wang, J., & Wu, G. (2016). Estimation of arsenic in agricultural soils using hyperspectral vegetation indices of rice. *Journal of hazardous materials*, 308, 243-252.
- [14] Cai, Z., Lei, S., Zhao, Y., Gong, C., Wang, W., & Du, C. (2022). Spatial Distribution and Migration Characteristics of Heavy Metals in Grassland Open-Pit Coal Mine Dump Soil Interface. *International Journal of Environmental Research and Public Health*, 19(8), 4441.
- [15] Tian, S., Wang, S., Bai, X., Zhou, D., Luo, G., Yang, Y., ... & Lu, Q. (2020). Ecological security and health risk assessment of soil heavy metals on a village-level scale, based on different land use types. *Environmental geochemistry and health*, 42(10), 3393-3413.
- [16] Alzahrani, D. A., Selim, E. M. M., & El-Sherbiny, M. M. (2018). Ecological assessment of heavy metals in the grey mangrove (*Avicennia marina*) and associated sediments along the Red Sea coast of Saudi Arabia. *Oceanologia*, 60(4), 513-526.
- [17] Shi, T., Liu, H., Wang, J., Chen, Y., Fei, T., & Wu, G. (2014). Monitoring arsenic contamination in agricultural soils with reflectance spectroscopy of rice plants. *Environmental science & technology*, 48(11), 6264-6272.
- [18] Amigo, J. M., & Santos, C. (2020). Preprocessing of hyperspectral and multispectral images. In *Data Handling in Science and Technology (Vol. 32, pp. 37-53)*. Elsevier.
- [19] Jia, J., Wang, Y., Chen, J., Guo, R., Shu, R., & Wang, J. (2020). Status and application of advanced airborne hyperspectral imaging technology: A review. *Infrared Physics & Technology*, 104, 103115.
- [20] Vidal, M., & Amigo, J. M. (2012). Pre-processing of hyperspectral images. Essential steps before image analysis. *Chemometrics and Intelligent Laboratory Systems*, 117, 138-148.
- [21] Medus, L. D., Saban, M., Francés-Víllora, J. V., Bataller-Mompeán, M., & Rosado-Muñoz, A. (2021). Hyperspectral image classification using CNN: Application to industrial food packaging. *Food Control*, 125, 107962.
- [22] Asad, M. H., & Bais, A. (2020). Weed detection in canola fields using maximum likelihood classification and deep convolutional neural network. *Information Processing in Agriculture*, 7(4), 535-545.

- [23] Liang, M., Jiao, L., & Meng, Z. (2019). A superpixel-based relational auto-encoder for feature extraction of hyperspectral images. *Remote Sensing*, 11(20), 2454.
- [24] Yang, X., Ye, Y., Li, X., Lau, R. Y., Zhang, X., & Huang, X. (2018). Hyperspectral image classification with deep learning models. *IEEE Transactions on Geoscience and Remote Sensing*, 56(9), 5408-5423.
- [25] Liu, B., Yu, A., Zuo, X., Xue, Z., Gao, K., & Guo, W. (2021). Spatial-spectral feature classification of hyperspectral image using a pretrained deep convolutional neural network. *European Journal of Remote Sensing*, 54(1), 385-397.
- [26] Liu, P., Liu, Z., Hu, Y., Shi, Z., Pan, Y., Wang, L., & Wang, G. (2019). Integrating a Hybrid Back Propagation Neural Network and Particle Swarm Optimization for Estimating Soil Heavy Metal Contents Using Hyperspectral Data. *Sustainability*, 11(2), 419.
- [27] A. K. Agarwal, D. Ather, R. Astya, D. Parygin, A. Garg and D. Raj, "Analysis of Environmental Factors for Smart Farming: An Internet of Things Based Approach," 2021 10th International Conference on System Modeling & Advancement in Research Trends (SMART), 2021, pp. 210-214, doi: 10.1109/SMART52563.2021.9676305.
- [28] A. K. Agarwal, M. Anam, D. K. Sharma, R. Regin, M. Acharya and K. Ashok, "Application of Access Control Framework in Cloud Reliability," 2021 2nd International Conference on Smart Electronics and Communication (ICOSEC), 2021, pp. 1-5, doi: 10.1109/ICOSEC51865.2021.9591973.
- [29] A. K. Agarwal, R. G. Tiwari, R. K. Kaushal and N. Kumar, "A Systematic Analysis of Applications Of Blockchain in Healthcare," 2021 6th International Conference on Signal Processing, Computing and Control (ISPCC), 2021, pp. 413-417, doi: 10.1109/ISPCC53510.2021.9609339.
- [30] R. G. Tiwari, A. K. Agarwal, R. K. Kaushal and N. Kumar, "Prophetic Analysis of Bitcoin price using Machine Learning Approaches," 2021 6th International Conference on Signal Processing, Computing and Control (ISPCC), 2021, pp. 428-432, doi: 10.1109/ISPCC53510.2021.9609419.
- [31] Agarwal, A.K., Rani, L., Tiwari, R.G., Sharma, T., Sarangi, P.K. (2021). Honey Encryption: Fortification Beyond the Brute-Force Impediment. In: Manik, G., Kalia, S., Sahoo, S.K., Sharma, T.K., Verma, O.P. (eds) *Advances in Mechanical Engineering. Lecture Notes in Mechanical Engineering*. Springer, Singapore. https://doi.org/10.1007/978-981-16-0942-8_64
- [32] R. K. Jindal, A. K. Agarwal, and A. K. Sahoo, "Data analytics for analysing traffic accidents," *Test Eng. Manag.*, vol. 83, no. 14796, 2020.
- [33] R. K. Jindal, A. K. Agarwal, and A. K. Sahoo, "Envisaging the road accidents using regression analysis," *Int. J. Adv. Sci. Technol.*, vol. 29, no. 5 Special Issue, pp. 1708–1716, 2020.
- [34] T. Agrawal, A. K. Agrawal, and S. K. Singh, "Cloud sanctuary through effectual access control and cryptographic model," *J. Adv. Res. Dyn. Control Syst.*, vol. 11, no. 6, pp. 533–537, 2019.
- [35] Tiwari, R.G., Pratibha, Dubey, S., Agarwal, A.K. (2023). Impact of IDMA Scheme on Power Line Communication. In: Deepak, B., Bahubalendruni, M.R., Parhi, D., Biswal, B.B. (eds) *Recent Trends in Product Design and Intelligent Manufacturing Systems. Lecture Notes in Mechanical Engineering*. Springer, Singapore. https://doi.org/10.1007/978-981-19-4606-6_90
- [36] Dutta, S. et al. (2023). Forecasting the Growth in Covid-19 Infection Rates. In: Dutta, P., Chakrabarti, S., Bhattacharya, A., Dutta, S., Piuri, V. (eds) *Emerging Technologies in Data Mining and Information Security. Lecture Notes in Networks and Systems*, vol 491. Springer, Singapore. https://doi.org/10.1007/978-981-19-4193-1_66
- [37] K. . Agarwal, V. . Kiran, R. K. . Jindal, D. . Chaudhary, and R. G. . Tiwari, "Optimized Transfer Learning for Dog Breed Classification", *Int J Intell Syst Appl Eng*, vol. 10, no. 1s, pp. 18–22, Oct. 2022.
- [38] Ambuj Kumar Agarwal, Gulista Khan, Shamimul Qamar, Niranjana Lal, Localization and correction of location information for nodes in UWSN-LCLI, *Advances in Engineering Software*, Volume 173, 2022, 103265, ISSN 0965-9978, <https://doi.org/10.1016/j.advengsoft.2022.103265>.